Sensing and Bio-Sensing Research 26 (2019) 100298

Contents lists available at ScienceDirect

Sensing and Bio-Sensing Research

journal homepage: www.elsevier.com/locate/sbsr

A low-cost and highly integrated sensing insole for plantar pressure measurement

Qi Zhang[a], Yu Lu Wang[b], Yun Xia[c], Xuee Wu[a], Timothy Vernon Kirk[c], Xiao Dong Chen[a,c,*]

[a] Department of Chemical and Biochemical Engineering, Xiamen University, Fujian Province, China
[b] College of Energy, Xiamen University, Fujian Province, China
[c] School of Chemical and Environmental Engineering, College of Chemistry, Chemical Engineering and Material Science, Soochow University, Suzhou Industrial Park Campus, Jiangsu Province, China

ARTICLE INFO

Keywords:
Plantar pressure measurement
Highly integrated textile-only sensing insole
Capacitive pressure sensing insole
Low-cost
Antibacterial property
Gait phases (events)

ABSTRACT

Plantar pressure measurement plays an important role in monitoring health and sports performance. Here, instead of embedding force sensitive resistors in the insole, we developed a simple and low-cost, highly integrated, textile-only sensing insole for the measurement of plantar pressures. These sensors were composed entirely of fabric, and utilized a capacitive mechanism, with silver cloth as electrodes and cotton cloth as the dielectric element. The similarity of elasticity and flexibility between sensor and insole enabled them to be closely integrated, and avoided negative impact on comfort. Additionally, the silver cloth electrodes contributed good antibacterial properties. The sensors exhibited fast response, negligible hysteresis, high sensitivity (0.947 MPa^{-1}), and good stability. Based upon capacitive responses to plantar pressures from the instrumented insole, gait phases (events) in different patterns were detected, giving the potential to monitor the health of the foot.

1. Introduction

Plantar pressure measurement is crucial for health and sports performance monitoring in areas such as gait phase detection [1–5], diabetic foot ulcers [6–8], flat-feet study [9–11], and sprint acceleration performance [12–14]. The most commonly used sensing devices for these measurements are generally categorized as plantar pressure platform systems [7–14] and sensing insoles systems [1–6].

Compared with platform systems, sensing insoles are more attractive because of their wearability, which allows the patient to use them outside of the clinic for continuous data logging [15,16]. Sensing insoles can measure plantar pressures by the embedded pressure sensors [17], with commercial force sensitive resistors (FSRs) dominating the market for the pressure sensing elements [1–5,18,19] until recently. Fig. 1a illustrates the details of a widely used force sensitive resistor (Interlink Electronics Inc., America, FSR® 402). The FSRs are good at sensing pressures, but are not outstandingly accurate, and are not suitable for precision measurement as load cells or strain gauges [3,5,20]. Their typical incorporation methods into the insole, fixing with adhesive [2,3,18] or embedding [4,5], can't ensure a high level of integration between sensor and insole. Additionally, the FSRs are made of robust and relatively thick polymer films comprised of polyetherimide, polyethersulfone, or polyester [20], which have different mechanical properties to native footwear insoles. This lack of integration, and dissimilarity of materials between sensors and insoles, can lead to poor effects on comfort and wearability, and looseness or delamination of sensors from insoles during long-term wear.

In this study, a textile-only, capacitive pressure sensing insole was developed with a high degree of sensor integration, due to the textile construction of both sensors and insoles. The fabrication process is both simple and low-cost, which derives from the all-cloth materials. As shown in Fig. 1b, by inserting two layers of conductive silver cloth into the multi-layer structure of a cloth insole, the sensing insole is fabricated. The conductive silver cloth layers sandwich four layers of cotton cloth, which are used as electrodes and dielectric respectively. The advantages of the capacitive design contribute to the good performance of textile-based sensors in signal response, hysteresis, and stability. Further, the conductive silver cloth not only acts as electrodes, but also provide a good antibacterial property, which is an important consideration for the wearable devices intended for long-term use. Three

* Corresponding author at: School of Chemical and Environmental Engineering, College of Chemistry, Chemical Engineering and Material Science, Soochow University, Suzhou Industrial Park Campus, Jiangsu Province, China
E-mail addresses: 20620140153872@stu.xmu.edu.cn (Q. Zhang), 20154009042@stu.suda.edu.cn (Y. Xia), tim@suda.edu.cn (T.V. Kirk), xdchen@mail.suda.edu.cn (X.D. Chen).

https://doi.org/10.1016/j.sbsr.2019.100298
Received 29 April 2019; Received in revised form 29 August 2019; Accepted 9 September 2019

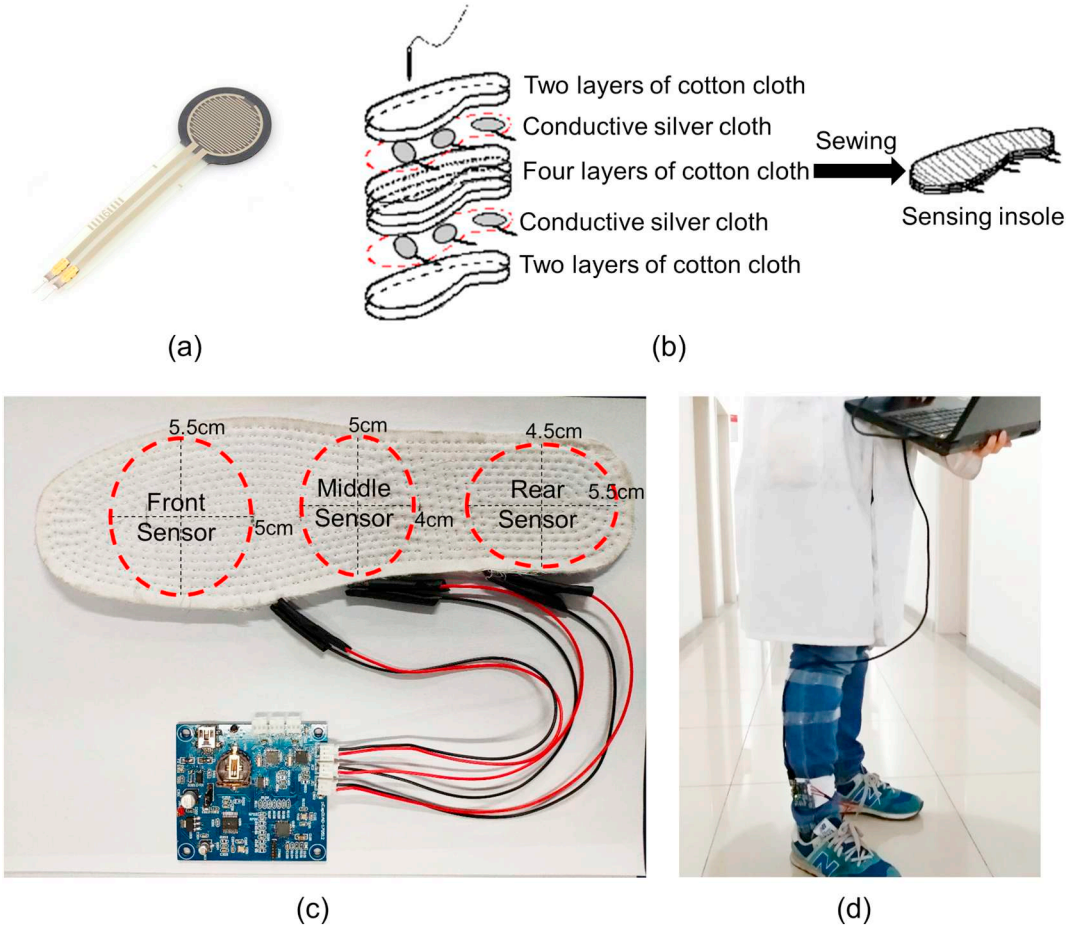

Fig. 1. (a) A widely used force sensitive resistor (Interlink Electronics Inc., America, FSR® 402 [20]); (b) Fabrication process for textile-only, capacitive pressure sensing insole; (c) Sensor layout of the textile-only, capacitive pressure sensing insole, shown connected to data acquisition system; (d) Digital photo of subject wearing sensing insole connected to data acquisition system.

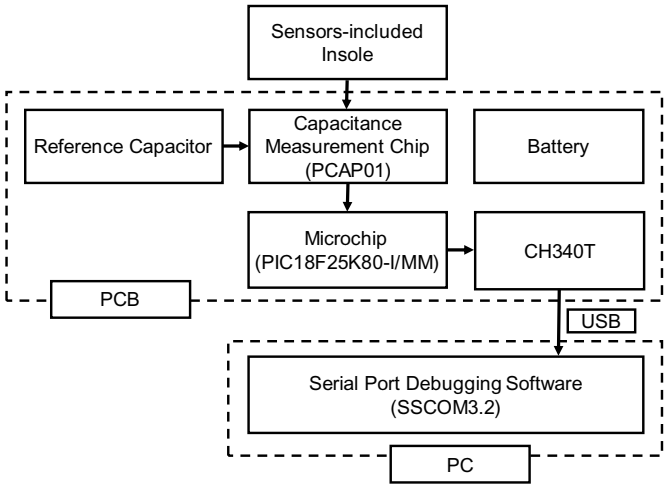

Fig. 2. The block diagram of the insole sensing system.

textile-based capacitive sensors are integrated in the front, middle and rear of the insole to measure the plantar pressures (Fig. 1c, hereafter referred to the front sensor, the middle sensor and the rear sensor). This sensing insole system, where the instrumented insole was connected with a portable capacitive measurement circuit and laptop, was applied to real-time gait phase detection for monitoring of foot health.

2. Materials and methods

2.1. Fabrication of sensing insole

The insole demonstrated in the paper is fabricated with a process shown in Fig. 1b. Firstly, the cotton cloth is cut into the shape of the insole, the size of which is US 8. Then, the conductive silver cloth is divided into three ellipses as the electrodes for three capacitive sensors in the front, middle and rear of the insole, with dimension parameters of 5.5 cm × 5 cm, 5 cm × 4 cm, 5.5 cm × 4.5 cm respectively. It is noted that each ellipse should have a strip as a conducting wire which can be linked to the micro measuring circuit. The layout of the sensors is depicted in Fig. 1c. Lastly, the cotton cloth and the conductive silver cloth are stitched together for an insole with a needle and thread. From top to bottom, in sequences, are two layers of cotton cloth, conductive silver cloth, four layers of cotton cloth, conductive silver cloth and two layers of cotton cloth. The simple layout can cover the important plantar pressure distribution areas such as ball of foot, arch of foot and the heel.

2.2. Design of insole sensing system

The block diagram of the insole sensing system is shown in Fig. 2. The capacitances of sensors in the insole are measured by a Capacitance Measurement Chip (PCAP01). The chip can obtain the ratio of testing capacitor and reference capacitor by comparing their charging and discharging time. The ratio is converted to the capacitance of the testing capacitor by the Microchip (PIC18F25K80-I/MM) and then transmitted

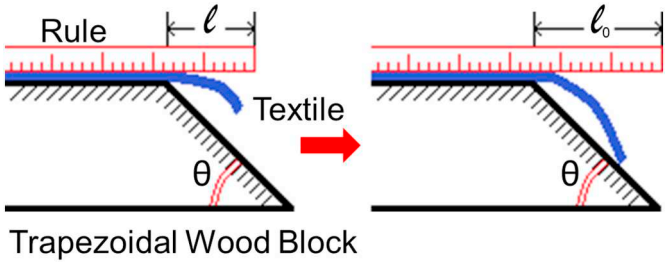

Fig. 3. The detection platform for determination of bending behavior of textiles.

to the computer by USB cable (the Bluetooth module is being developed). Data Acquisition and Control is carried out by a Serial Port Debugging Software (SSCOM3.2).

2.3. Microstructure characterization of the electrode of silver cloth

Morphological characterization in this study was carried out with a Hitachi SU1510 (Hitachi High-Technologies Corporation, Japan) SEM. A Bruker energy dispersive spectrometer (XFlash 6130, Bruker Corporation, USA) connected to the microscope was employed to observe element distribution on surfaces.

2.4. Determination of bending behavior of textiles

Softness of textiles is an important index for wearing comfort, which is usually evaluated by its opposite characteristics—bending strength. The bending strengths of cotton cloth and silver cloth used in the sensing insole were tested on a homemade detection platform as shown in Fig. 3. Bending strength was assessed in accordance with incline method from the Chinese Standard GB/T 18318.1–2009 (*Textiles–determination of bending behavior–Part 1:Incline method*). The size of the samples was (25 ± 1) mm × (250 ± 1) mm. The long side of the sample of silver cloth was parallel to the transverse direction of the fabric (see Fig. 4, X-axis direction). The samples were taken at least 100 mm away from the edges of the fabric and touched as little as possible by hand. As shown in Fig. 3, the long and narrow samples were placed on the surface of trapezoidal wood block. The angle between inclined plane and horizontal line was 45°. A ruler with rubber layer on the bottom was pressed on the sample, where the top of the ruler was even with the sample. Then the sliding ruler was pushed out slowly at a certain speed (0.1 cm/s). The sample slid out synchronously under the driving of the ruler, and drooped toward inclined plane due to its own weight. When the top of the sample had just touched the inclined plane, the length of the sample sliding out was read out from the ruler. The bending length and bending strength of the samples were calculated according to the Eqs. (1) and (2).

$$C = L\bullet\left[\frac{\cos\frac{\theta}{2}}{8\tan\theta}\right]^{\frac{1}{3}}, \quad (1)$$

where C, L, θ is the bending length of the sample (cm), the length of the sample sliding out (cm), the angle between inclined plane and horizontal line (°), respectively.

$$G = m' \times C^3 \times 10^{-3}, \quad (2)$$

where G, m′ is the bending strength per unit width of the sample (mN•cm), the mass per unit area (g/m^2), respectively.

2.5. Pressure-capacitance behavior tests of textile-based sensors

The pressure-capacitance behavior tests of textile-based sensors were carried out on a texture analyzer (BROOKFIELD, America, CT3 50 K) with a fixture base (TA-BT-KIT) and probe (TA 25/1000). The parameters were set as follows: Test type: Compression, Trigger load: 10 g, Pretest speed: 1 mm/s, Test speed: 0.1 mm/s, Return speed: 0.1 mm/s.

2.6. Bacterial resistance tests

E. coli (ATCC29522) was selected as the model species for characterizing insole bacterial resistance. Antibacterial activity was assessed in accordance with the shake flask test from the Chinese Standard GB/T 20944.3-2008 [21,22] (*Textiles–Evaluation for antibacterial activity–Part 3:Shake flask method*). 0.75 g sample (all the samples without any treatment) was cut into small pieces of dimensions around 5 × 5 mm^2, which were sterilized for 15 min under the condition of 103 kPa and 125 °C in the autoclave sterilizer. They were taken out and put in sterilized conical flasks for air cooling. A fresh bacterial suspension was first acquired by culturing *E. coli* in 20 mL of autoclaved broth (Sinopharm Chemical Reagent Ltd., 3 g/L beef extract, 5 g/L peptone) at 37 °C for 20 h after inoculation; the rotation speed was 130 rpm. Subsequently, 2 mL of the bacterial suspension was removed and diluted in autoclaved broth and buffer solution (PBS, 0.03 mol/L, pH = 7.2–7.4) to reach a concentration of about 3 × 10^5 CFU/mL for the sterilization test. Then 5 mL of the diluted bacterial solution was placed into an autoclaved conical flask (containing 0.75 g of sample and 70 mL of PBS) at 24 °C for 18 h; the rotation speed was 150 rpm. Finally, 1 mL of the bacterial solution from the conical flask was spread evenly on agar dishes (Sinopharm Chemical Reagent Ltd., 3 g/L beef extract, 5 g/L peptone, 15 g/L agar), incubated for 24 h at 37 °C. The photos of colonies on the surface of dishes were took with colony counter (Shineso Ltd., Hang Zhou City, China, Czone 5F).

2.7. Gait phase detection

The author of this paper (Qi Zhang), who had normal gait with no

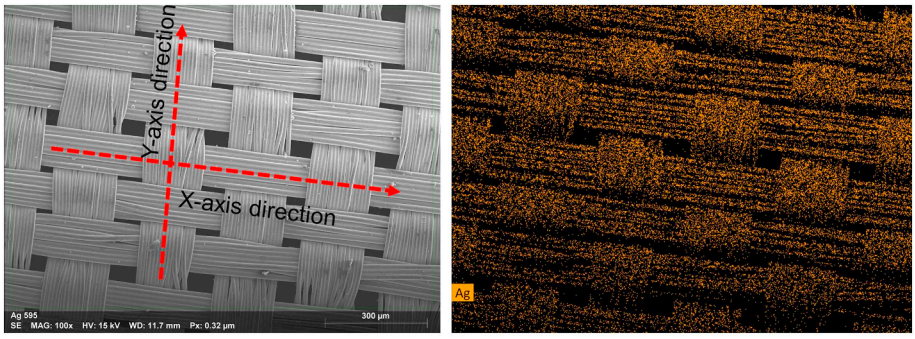

(a) (b)

Fig. 4. SEM and EDS images of the surface of silver cloth.

Table 1
The thicknesses and bending strengths of the cotton cloth and silver cloth used in the sensing insole respectively.

Materials	Thickness	Bending length	Bending strength
Cotton cloth	0.40 mm	1.70 cm	0.7409 mN.cm
Silver cloth	0.05 mm	1.51 cm	0.1817 mN.cm

pathologies that would influence his gait patterns, was enrolled in this study at laboratory. The subject wore the shoes with sensing insoles for gait phase detections during waking hours. No instruction was provided for specific tasks, as the aim of this test was to assess natural living conditions and performance. The data of the two gait patterns in this study is unrepresentative, which are only used for evaluating the application of the sensing insole in gait phase detection.

3. Results and discussion

Fig. 4(a) and (b) show the SEM and EDS images of the silver cloth. The silver cloth is constituted by silver fibers based on the woven-structure. The EDS image shows that the silver cloth contains a large amount of deposited silver, which contributes to the good conductivity and the antibacterial property. Table S1, from the support information, shows that the silver cloth has a good conductivity and can keep it under compression. As shown in Table 1, the silver cloth is thinner than the cotton cloth used in insoles, and exhibits a smaller bending strength. The small bending strength indicates that the silver cloth is also soft. Due to the small thickness and good flexibility, adding silver cloth is not expected to affect the wearing comfort of insole. Furthermore, the wearing experiences that the author has had do not suggest the otherwise. The compression-load curves of the insole before and after inserting the silver cloth has also proved that the silver cloth will not cause any effect on compression performance of the insole. (see Fig. S1, the two almost overlapping results).

The large amount of deposited silver in silver cloth not noly contributes a good conductivity but also provide potential antibacterial properties [23,24]. As shown in Fig. 5a, two identical parts were cut from the insoles, which with and without silver cloth, and evaluated in the antibacterial tests. Compared with pure insole, the sensors-included insole presents a better antibacterial property as shown in Fig. 5b-d. Samples of the sensor-integrated insole prevented growth of bacteria in a shaker flask culture. This is shown in Fig. 5c, by the failure of the flask media to produce bacterial colonies when inoculating a culture plate. After wearing, it still maintains this property, as shown in Fig. 5d. It should be pointed out that the antibacterial properties of sensing insole are obtained by soaking samples in the culture solution, so the sensors-included insole maybe exhibit antimicrobial properties only when it is exposed to sweat, or it is being washed.

Fig. 6a shows the schematics of the structure of the sensing insole and the sensing mechanisms. The capacitances of the sensors in the sensing insole may be estimated using the following equation:

$$C = \varepsilon_0 \varepsilon_r \frac{A}{d}, \tag{3}$$

where ε_r, ε_0, A, d is the relative permittivity of the dielectric material (cotton cloth layers), the vacuum permittivity, the surface area of the electrodes (silver cloth layers), and the distance in between the two electrodes, respectively. When an external force is applied, the variation of surface area of electrodes may be neglected and the change in capacitance mainly comes from the compression of the cotton interlayers.

$$\frac{C}{C_0} = \frac{d_0}{d}, \tag{4}$$

Co is the reference or the original capacitance. do is the original distance between electrodes. Three textile-based capacitive sensors are integrated in the front, middle and rear locations of the insole respectively, as shown in Fig. 6a, where they share the same cotton interlayers. Under the same pressure, the compression ratio of the dielectric

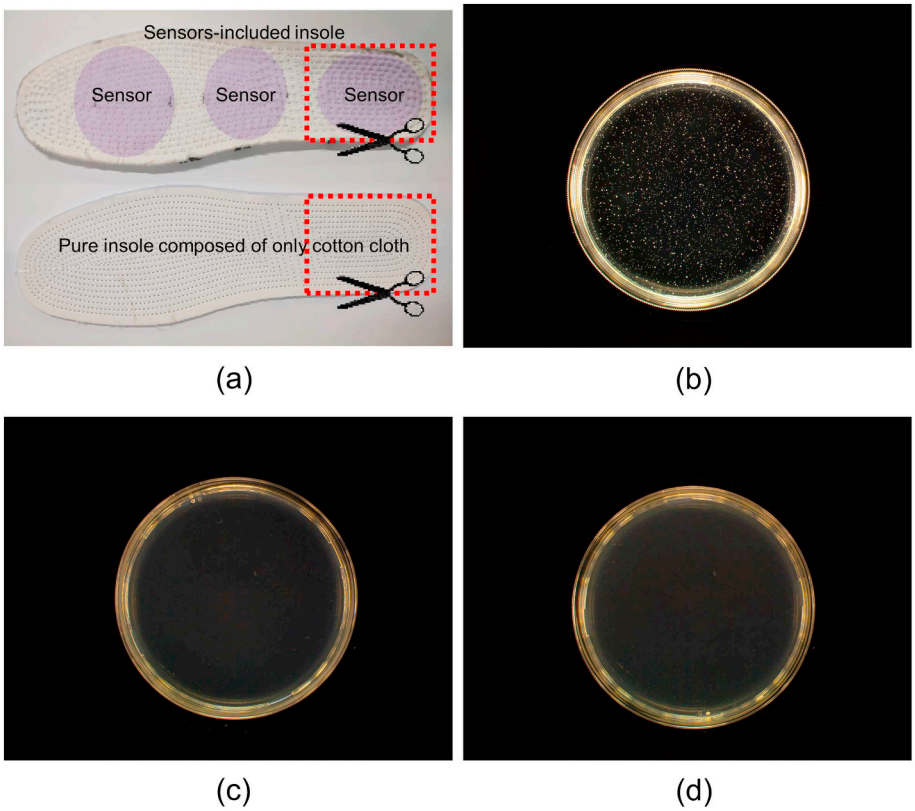

Fig. 5. (a) The samples were cut from the pure insole and sensing insole, respectively. (b-d) Photographs of *Escherichia coli* colonies in the antibacterial tests. The colonies on the surface of dishes are from shaker flasks which contain bacterial solution and different samples. (b) Pure insole composed of only cotton cloth. The shaker flask containing pure insole is used as the positive control for bacterial growth; (c) Original sensors-included insole; (d) The sensors-included insole after wearing for a month.

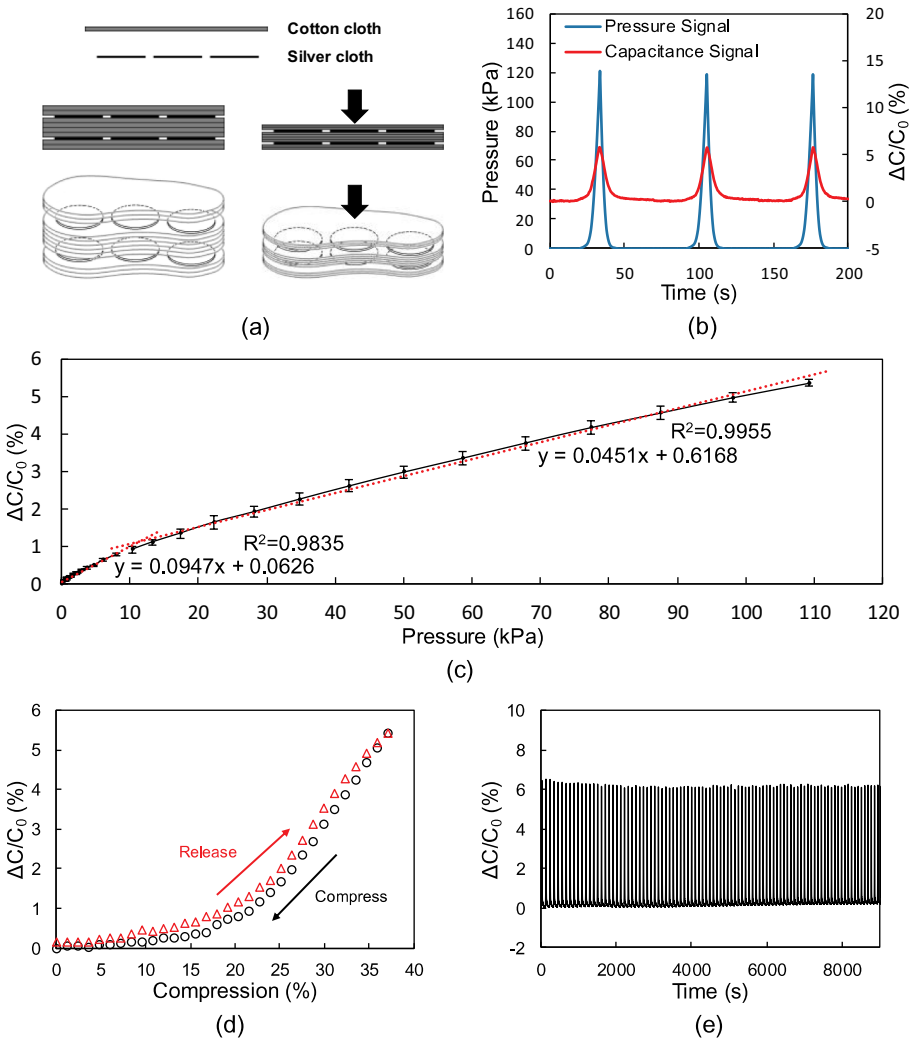

Fig. 6. (a) Schematics of the structure of the sensing insole and the sensing mechanisms based on the capacitance changes monitored for the pressure changes (the changes of the displacement between each pair of the electrodes) induced by plantar movement. The silver cloth were made up as the electrodes in three pairs which were imbedded into the cotton cloth assembly; (b) Continuous capacitance and pressure signals of the sensing insole; (c) Relationship between capacitances and pressures of the sensing insole; (d) Capacitance change of the sensing insole from a consecutive linear compress-release cycle of compression; (e) Capacitive responses of the sensing insole to repeated compress-release cycles in a 40% compression.

Table 2
Summary of the performance of wearable pressure sensors reported in the literature.

Materials	Type of sensor	Sensitivity	Detection limit	Ref.
Gold thin films-Silicone rubber	Capacitive	0.4 MPa^{-1} in the range up to 160 kPa	~30 kPa	[25]
Conductive PDMS-Ecoflex	Capacitive	0.417 MPa^{-1} in the range up to 1.2 MPa	50 kPa	[26]
Au thin layers-Ecoflex	Capacitive	0.48 MPa^{-1} in the range up to 0.25 MPa	~25 kPa	[27]
CNT film-Ecoflex	Capacitive	0.23 MPa^{-1} in the range up to 1 MPa	~50 kPa	[28]
Conductive rubber-Carbon black/silicone rubber dielectric	Capacitive	0.2536 MPa^{-1} in the range up to 700 kPa	~25 kPa	[29]
AgNW/PU-Acrylic elastomeric dielectric spacer	Capacitive	0.51 MPa^{-1} in the range up to 1 MPa	~20 kPa	[30]
Silver cloth layers-Cotton cloth layers	Capacitive	0.947 MPa^{-1}, 0–10 kPa;0.451 MPa^{-1}, 10 kPa ~ 200 kPa	~1 kPa	This work

layer of the three sensors is the same, so the rates of change in capacitance of the three sensors should be the same according to Eq. (4). Hence, the three capacitive sensors in different positions of the sensing insole have the same pressure-capacitance curves (Y-axis is the change rate of capacitance). The pressure measurements of the sensing insole are based on the pressure-capacitance curves.

Once again, these pressure responses are recorded as the capacitance curves which represent the plantar compressive and reflective movements.

Fig. 6b-e shows the sensing performance of the sensing insole. Fig. 6b shows that the capacitances of the sensing insole are responsive to pressures applied on the insole with no obvious hysteresis. The pressure-capacitance curves are shown in Fig. 6c and the fitting equations are as follows:

$$Y = 0.0947\,X + 0.0626,\ X < 10\ \text{kPa} \quad (5)$$

$$Y = 0.0451\,X + 0.6168,\ X \geq 10\ \text{kPa} \quad (6)$$

The sensitivity of capacitive pressure sensors, S, can be defined as the slope of the traces ($S = \delta(\Delta C/C_0)/\delta p$, where p is the applied pressure, while C and C_0 are the capacitances with and without the applied pressure, respectively). For pressures below and above 10 kPa, the sensitivity of our sensors is 0.947 MPa^{-1} and 0.451 MPa^{-1}, respectively. The sensitivity is higher than many previously reported wearable capacitive pressure sensors [25–30]. For example, a sensor with conductive PDMS as electrodes and Ecoflex as dielectric, reported by Woo et al. [26], exhibited a sensitivity of 0.417 MPa^{-1} in the range up to 1.2 MPa. A sensor with CNT films as electrodes and Ecoflex as dielectric, reported by Lipomi et al. [28], exhibited sensitivity of 0.23 MPa^{-1}. For pressures in the range up to 700 kPa, a sensor based on

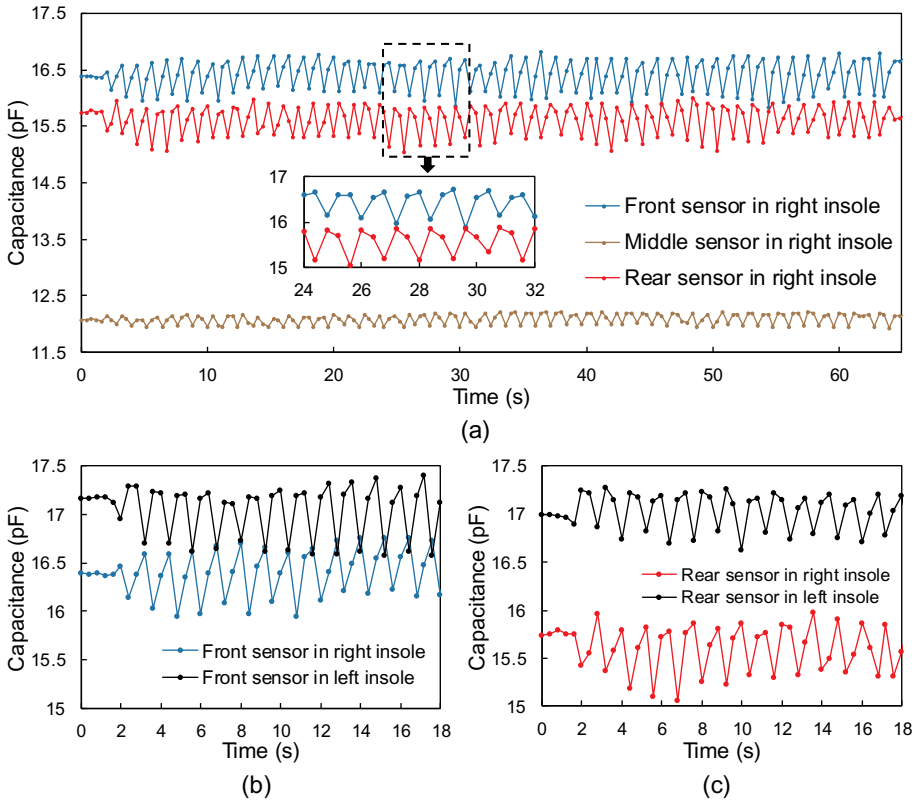

Fig. 7. (**a**) Walking signals from the sensors in right insole; (**b**,**c**) The comparisons between walking signals of right and left feet. (**b**) From front sensors; (**c**) From rear sensors.

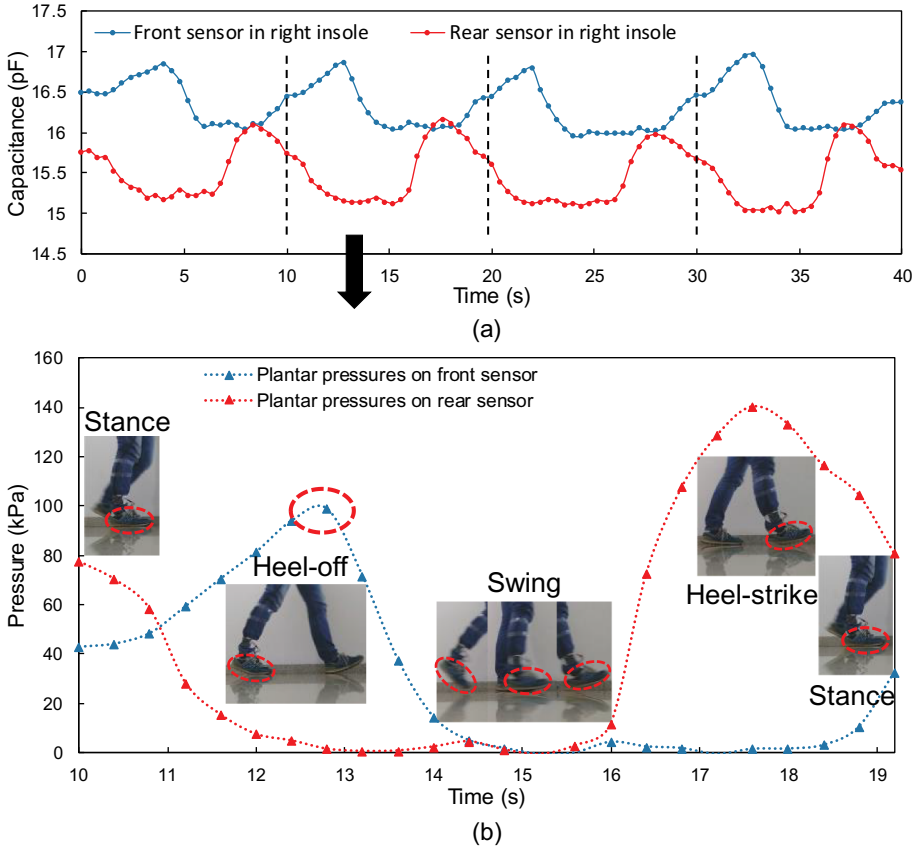

Fig. 8. (**a**) Capacitive signals of the slow motion of walking composed of four steps; (**b**) The simulated time-pressure curves of plantar pressures during a gait cycle: stance, heel-off, swing and heel-strike.

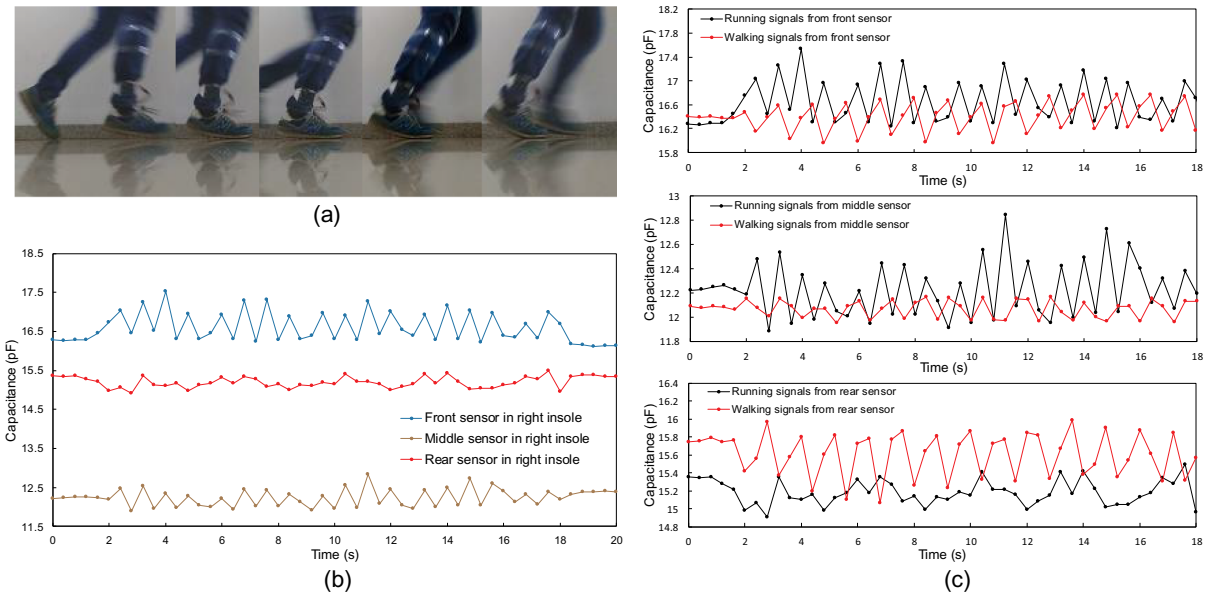

Fig. 9. (**a**) Digital photos of the running gait; (**b**) Running signals from the sensors in right insole; (**c**) Comparisons between the running signals and walking signals.

a textile substrate with carbon black/silicone rubber composite dielectric, reported by Guo et al. [29], exhibited a sensitivity of 0.2536 MPa^{-1}. Characteristics of comparable capacitive pressure sensors are summarized in Table 2.

Fig. 6d presents capacitance changes of the sensing insole from a consecutive linear compress-release cycle of compression. A negligible hysteresis is observed in Fig. 6d. And the output signals of the sensing insole are stably maintained without any remarkable degradation in repeated cycling tests (Fig. 6e).

Fig. 7a shows the walking signals recorded by the sensing insole system (normal walking speed, 0.8–0.9 m/s). The number of walking steps are recorded clearly. The amplitudes of signals can accurately reflect the stress condition between floor and different parts of foot, which can be used in the monitoring of foot health. For example, if there is a remarkable and long-term increase or decrease in the signal amplitude of the middle sensor, it might be caused by flat foot or cavus foot.

After comparing walking signals between right and left feet, it is found that the peaks of signals are staggered from each other as shown in Fig. 7b, c, which clearly reflects the alternating forward motions of the feet. It should be noticed that the motion resolution is constrained by the sampling frequency (2.5 Hz) of the measurement circuit, rather than the inherent response characteristics of the textile-based sensors.

The fabricated sensing system was implemented in the real-time application of gait phases detection. The capacitive signals of walking gait from front sensor and rear sensor are shown in Fig. 8 (restricted by the sampling frequency of measuring circuit, the gait signals were collected from the slow motion of walking, the speed was about 0.13 m/s). Fig. 8b shows the simulated time-pressure curves of plantar pressures during a gait cycle: stance, heel-off, swing and heel-strike, which were simulated according to the relationship between capacitance and applied pressure (Eqs. (5) and (6)). The simulative results were in good agreement with the actual plantar pressures during walking process. The transitions of gait are shown below:

(1) stance → heel-off: In this transition, the forefoot was in contact with the ground and the heel gradually rose from the ground. The forefoot provided the power constantly instead of the heel. Therefore, the pressure on the front sensor increased gradually, while that on the rear sensor was reduced to zero.
(2) heel-off → swing: In this transition, the tester's foot gradually lost the contact with the ground when toes lift off, which led to the zero pressure on the front sensor.
(3) swing → heel-strike: When the foot swung in the air, it had no contact with the ground, so the pressures on the front and rear sensors were nearly zero.
(4) heel-strike → stance: During this transition, the heel touched the ground firstly, then the whole foot. Therefore, the heel experienced a high impact force acting as a buffer, and the pressure on the rear sensor increased rapidly. Then the forefoot touched the ground and the weight was transferred to the entire foot. So, the pressures on the front and rear sensors turned to the "initial value" (the values in stance phase).

At the "heel-off" gait phase, before the peak of the pressure, only one forefoot contacts with the ground and provides the support of the weight of the body, while the another foot is at the "free swing" gait phase. From Fig. 8b, the pressure under the forefoot is 100 kPa at the peak, and the stressed area of forefoot at this point is 0.00845 m2, which is about half of the insole area. According to the force formula ($F = P \times S$, where P is the pressure under the forefoot and S is the stressed area of the forefoot), it can be calculated that the bodyweight is 845 N (84.5 kg), which is close to the real weight of the tester person (80 kg).

Another gait pattern is tested as shown in Fig. 9, when the heel trys not to touch the ground and the power mainly comes from the front and middle part of the foot. The posture is usually used in the running for the tester(the data of the gait patterns are unrepresentative, which are only used for evaluating the sensing insole system). As shown in Fig. 9c, there are distinct differences in capacitive responses of sensors between this running pattern and previous walking pattern, which indicates that the insole sensing system can differentiate the two patterns. The capacitive signals from the rear sensor are below the initial value in most time due to the less contact between heel and ground, and the signal amplitude of the middle sensor has an obvious increase because the middle part of foot is active in the movement.

4. Conclusions

A low-cost, effective, antibacterial, and textile-only, capacitive pressure sensing insole has been developed, which combines a simple fabrication process with a high degree of sensor integration. The sensor

elements were formed by sandwiching a cotton cloth dieletric layer between silver cloth electrodes. As the sensor and the insole materials are both composed of fabric, they have similar compliant mechanical properties, facilitating comfort and wearability. Good sensing performance and stability was exhibited, which was combined with antibacterial properties from the silver elements. By integrating three sensors per insole, the distribution of plantar pressures could be measured during gait cycles, with test results conforming to those expected during gait phase detection. Based on the advantages of low-cost materials and facile fabrication, degree of sensor integration, comfort, and antibacterial properties, the textile-only sensing insole may provide new opportunities for furthering the adoption and development of systems for monitoring plantar pressure during patient locomotion, or during athletic performance.

Declaration of Competing Interest

All the authors declare that there is no conflict of interest.

Acknowledgements

The current work was partially funded through Professor Xiao Dong Chen's setup grant at Soochow University.

Appendix A. Supplementary data

Supplementary data to this article can be found online at https://doi.org/10.1016/j.sbsr.2019.100298.

References

[1] M.M. Skelly, H.J. Chizeck, Real-time gait event detection for paraplegic FES walking, IEEE Trans. Neural Syst. Rehab. Eng. 9 (2002) 59–68.
[2] K. Tee, Y.S.H. Javahar, I.S. Hashim, W.N. Wan Zakaria, S. Mohd Khialdin, H. Isa, M. Awad, C. Soon, A portable insole pressure mapping system, TELKOMNIKA. 15 (2017) 1493–1500.
[3] I.P.I. Pappas, M.R. Popovic, T. Keller, V. Dietz, M. Morari, A reliable gait phase detection system, IEEE Trans. Neural Syst. Rehab. Eng. 9 (2001) 113–125.
[4] S.J.M. Bamberg, A.Y. Benbasat, S. Donna Moxley, D.E. Krebs, J.A. Paradiso, Gait analysis using a shoe-integrated wireless sensor system, IEEE Trans. Inf. Technol. Biomed. 12 (2008) 413–423.
[5] I.P.I. Pappas, T. Keller, S. Mangold, M.R. Popovic, V. Dietz, M. Morari, A reliable gyroscope-based gait-phase detection sensor embedded in a shoe insole, IEEE Sensors J. 4 (2004) 268–274.
[6] S.A. Bus, J.S. Ulbrecht, P.R. Cavanagh, Pressure relief and load redistribution by custom-made insoles in diabetic patients with neuropathy and foot deformity, Clin. Biomech. 19 (2004) 629–638.
[7] A. Caselli, H. Pham, J.M. Giurini, D.G. Armstrong, A. Veves, The forefoot-to-rearfoot plantar pressure ratio is increased in severe diabetic neuropathy and can predict foot ulceration, Diabetes Care 25 (2002) 1066–1071.
[8] L.A. Lavery, D.G. Armstrong, R.P. Wunderlich, J. Tredwell, A.J. Boulton, Predictive value of foot pressure assessment as part of a population-based diabetes disease management program, Diabetes Care 26 (2003) 1069–1073.
[9] J. Pauk, J. Griškevičius, Ground reaction force and support moment in typical and flat-feet children, Mechanika. 17 (2011) 93–96.
[10] A.K. Buldt, S. Forghany, K.B. Landorf, G.S. Murley, P. Levinger, H.B. Menz, Centre of pressure characteristics in normal, planus and cavus feet, J. Foot Ankle Res. 11 (2018) 3.
[11] A.K. Buldt, S. Forghany, K.B. Landorf, P. Levinger, G.S. Murley, H.B. Menz, Foot posture is associated with plantar pressure during gait: a comparison of normal, planus and cavus feet, Gait Posture 62 (2018) 235–240.
[12] R. Nagahara, M. Mizutani, A. Matsuo, H. Kanehisa, T. Fukunaga, Step-to-step spatiotemporal variables and ground reaction forces of intra-individual fastest sprinting in a single session, J. Sports Sci. 36 (2018) 1392.
[13] J.P. Hunter, R.N. Marshall, P.J. Mcnair, Relationships between ground reaction force impulse and kinematics of sprint-running acceleration, J. Appl. Biomech. 21 (2005) 31–43.
[14] G. Rabita, S. Dorel, J. Slawinski, E. Sàez-De-Villarreal, A. Couturier, P. Samozino, J.B. Morin, Sprint mechanics in world-class athletes: a new insight into the limits of human locomotion, Scand. J. Med. Sci. Sports 25 (2015) 583–594.
[15] J. Taborri, S. Rossi, E. Palermo, F. Patanè, P. Cappa, A novel HMM distributed classifier for the detection of gait phases by means of a wearable inertial sensor network, Sensors. 14 (2014) 16212–16234.
[16] M. Di Rosa, J.M. Hausdorff, V. Stara, L. Rossi, L. Glynn, M. Casey, S. Burkard, A. Cherubini, Concurrent validation of an index to estimate fall risk in community dwelling seniors through a wireless sensor insole system: a pilot study, Gait Posture 55 (2017) 6–11.
[17] C. Lou, C. Pang, C. Jing, S. Wang, X. He, X. Liu, L. Huang, F. Lin, X. Liu, H. Wang, Dynamic balance measurement and quantitative assessment using wearable plantar-pressure insoles in a pose-sensed virtual environment, Sensors. 18 (2018) 4193.
[18] X. Hu, J. Zhao, D. Peng, Z. Sun, X. Qu, Estimation of foot plantar center of pressure trajectories with low-cost instrumented insoles using an individual-specific nonlinear model, Sensors. 18 (2018) 421.
[19] M.D. Chang, E. Sejdić, V. Wright, T. Chau, Measures of dynamic stability: detecting differences between walking overground and on a compliant surface, Hum. Mov. Sci. 29 (2010) 977–986.
[20] Interlink Electronics Inc. USA, Force Sensing Resistor® Integration Guide and Evaluation Parts Catalog, https://www.sparkfun.com/datasheets/Sensors/Pressure/fsrguide.pdf, (2019) (accessed 24 April 2019).
[21] D. Zhang, G.W. Toh, H. Lin, In situ synthesis of silver nanoparticles on silk fabric with PNP for antibacterial finishing, J. Mater. Sci. 47 (2012) 5721–5728.
[22] X. Fu, Y. Shen, X. Jiang, D. Huang, Y. Yan, Chitosan derivatives with dual-antibacterial functional groups for antimicrobial finishing of cotton fabrics, Carbohydr. Polym. 85 (2011) 221–227.
[23] T. Dubas Stephan, Panittamat Kumlangdudsana, Pranut Potiyaraj, Layer-by-layer deposition of antimicrobial silver nanoparticles on textile fibers, Coll. Surf. A Physicochem. Eng. Aspects 289 (2006) 105–109.
[24] S.H. Jeong, Y.Y. Sang, S.C. Yi, The effect of filler particle size on the antibacterial properties of compounded polymer/silver fibers, J. Mater. Sci. 40 (2005) 5407–5411.
[25] D.P.J. Cotton, I.M. Graz, S.P. Lacour, A multifunctional capacitive sensor for stretchable electronic skins, IEEE Sensors J. 9 (2009) 2008–2009.
[26] S.J. Woo, J.H. Kong, D.G. Kim, J.M. Kim, A thin all-elastomeric capacitive pressure sensor array based on micro-contact printed elastic conductors, J. Mater. Chem. C 2 (2014) 4415–4422.
[27] Y. Ming, A.P. Bonifas, L. Nanshu, S. Yewang, L. Rui, C. Huanyu, A. Abid, H. Yonggang, J.A. Rogers, Silicon nanomembranes for fingertip electronics, Nanotechnology. 23 (2012) 344004.
[28] D.J. Lipomi, V. Michael, C.-K,.T. Benjamin, S.L. Hellstrom, J.A. Lee, C.H. Fox, B. Zhenan, Skin-like pressure and strain sensors based on transparent elastic films of carbon nanotubes, Nat. Nanotechnol. 6 (2011) 788–792.
[29] X. Guo, H. Ying, C. Xia, C. Liu, L. Ping, Capacitive wearable tactile sensor based on smart textile substrate with carbon black/silicone rubber composite dielectric, Meas. Sci. Technol. 27 (2016) 045105.
[30] W. Hu, X. Niu, R. Zhao, Q. Pei, Elastomeric transparent capacitive sensors based on an interpenetrating composite of silver nanowires and polyurethane, Appl. Phys. Lett. 102 (2013) 38–1487.